

# Spontaneous strain in quasi-two-dimensional Janus CdSe nanoplatelets and its microscopic mechanisms

Alexander I. Lebedev\*

Physics Department, Moscow State University, 119991 Moscow, Russia

(Dated: May 21, 2024)

Spontaneous strain and spontaneous folding of thin nanoplatelets are known phenomena whose microscopic mechanisms are still debating. In this work, first-principles calculations are used to study the mechanical stresses that arise in Janus CdSe nanoplatelets and result in their spontaneous strain. Calculations reveal the existence of three microscopic mechanisms of this phenomenon. Two bulk mechanisms are associated with the inverse piezoelectric effect in an electric field created by the difference in electronegativities of ligands and by the depolarizing field resulting from the difference in the potential jumps in electrical double layers on the surfaces of nanoplatelets. These mechanisms account for 5–25% of the observed effect. The third mechanism is associated with the surface strain of nanoplatelets by bridging bonds, and its influence is predominant. It is shown that the latter mechanism cause spontaneous folding of thin CdSe nanoplatelets and, depending on the values of surface stresses and lateral orientation of nanoplatelets, can result in formation of their experimentally observed structures such as scrolls, spirals, and twisted ribbons.

DOI: 10.1021/acs.jpcc.3c01934 (J. Phys. Chem. C 127, 9911 (2023))

## I. INTRODUCTION

Colloidal semiconductor nanoplatelets have been the topic of intense research in recent years [1–3]. Among them, nanoplatelets of cadmium chalcogenides have attracted much attention due to their outstanding optical properties. They are direct band gap semiconductors. Their perfectly defined thickness and strong quantum confinement in one direction result in extremely narrow emission and absorption lines [4]. Furthermore, they display giant oscillator strength [5], high quantum yield [1], short radiative recombination times, and very low lasing thresholds [6, 7], which can be used in a variety of optoelectronic applications.

An interesting feature of thin semiconductor nanoplatelets is their tendency to spontaneous folding [8]. This phenomenon has been most thoroughly studied in II–VI semiconductors. For example, in thin (2–4 monolayers) CdSe and CdTe nanoplatelets with zinc-blende structure and lateral sizes larger than 100 nm, it results in formation of scrolls [9–17], spirals (helicoids) [8, 16, 18, 19] as well as twisted ribbons [16, 20]. The diameter of the scrolls and spirals varies from 20 to 100 nm. Spontaneous folding slightly shifts the exciton absorption and luminescence bands to longer wavelengths, but can significantly reduce the luminescence quantum yield. An interesting feature of the above spiral and twisted structures is that they have chiral optical properties [17, 20, 21]. The occurrence of spontaneous folding has been attributed to an asymmetry of mechanical stresses created by surface ligands [10, 11, 14, 17], but its microscopic mechanism still remains questionable if one takes into account the perfect geometric symmetry of the semiconductor part

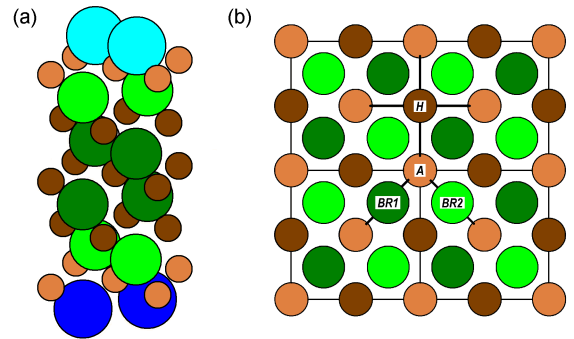


FIG. 1. (a) Structure of a 4 ML thick Janus CdSe nanoplatelet covered with two different monoatomic ligands (shown in cyan and blue). (b) Possible positions of ligands on the (001) surface of CdSe: atop (*A*), bridge(1) (*BR1*), bridge(2) (*BR2*), and hollow (*H*). Thick lines show the chemical bonds. The surface Cd atoms are shown in orange, other Cd atoms are brown, the Se atoms closest to surface are in green, and other Se atoms are dark green.

of nanoplatelets.

The aim of this work is a theoretical study of the phenomenon of spontaneous strain that arises in CdSe nanoplatelets when their two surfaces are covered with different ligands (Fig. 1a). Such nanoplatelets are called the Janus ones. In contrast to true Janus nanoplatelets like MoSSe [22] in which the real atomic substitution takes place, our Janus CdSe nanoplatelets retain their atomic structure, and the only change that is produced is the substitution of ligands. To the best of our knowledge, this is the first study of CdSe Janus nanoplatelets. Our interest to these objects stems from the fact that the strain that arises in them may be one of the cause of spontaneous folding of nanoplatelets. At the end of this article, experimental data supporting this hypothesis will be presented.

\* swan@scon155.phys.msu.ru

In this work, the microscopic mechanisms that result in spontaneous strain and spontaneous folding of Janus CdSe nanoplatelets will be established. The obtained results clarify the nature of physicochemical phenomena occurring at the interface between the nanoplatelet and surface ligands and show the ways to control the above phenomena.

## II. COMPUTATIONAL DETAILS

The objects of this study are the (001)-oriented CdSe nanoplatelets with zinc-blende structure. As was established in previous studies, [3, 15, 23] these nanoplatelets contain one excess atomic layer of cadmium, and two extra electrons from each Cd atom enter the conduction band. In order to bound these electrons and retain the semiconductor properties, two  $X$ -type ligands should be placed on both sides of the nanoplatelet.

The first-principles DFT calculations of the equilibrium geometry of nanoplatelets were carried out using the ABINIT software [24]. The local density approximation (LDA) and norm-conserving optimized pseudopotentials [25] constructed using the OPIUM program [26] were used in the calculations. The plane wave cutoff energy was 30 Ha (816 eV), the integration over the Brillouin zone was carried out on a  $8 \times 8 \times 8$  Monkhorst-Pack mesh for bulk CdSe and on a  $8 \times 8 \times 1$  Monkhorst-Pack mesh for nanoplatelets. The lattice parameters and the positions of atoms were relaxed until the forces acting on the atoms became less than  $5 \times 10^{-6}$  Ha/Bohr (0.25 meV/Å) while an accuracy of the total energy calculation was better than  $10^{-10}$  Ha.

The calculated lattice parameter of bulk zinc-blende CdSe was  $a = 6.0175$  Å, in good agreement with the experimental data of 6.077 Å [27] if one takes into account a small underestimation of the lattice parameter typical of the LDA. Under the tetragonal distortion, the FCC Bravais lattice of bulk CdSe transforms to body-centered tetragonal lattice, which loses some symmetry elements and transforms to a primitive tetragonal lattice when forming nanoplatelets. In this structure, the translation vectors are rotated by  $45^\circ$  relative to the axes of the original cubic cell, and the lattice parameters in the  $xy$  plane are  $a_0 = b_0 \approx a/\sqrt{2}$ . Our computations were performed on supercells, into which a vacuum gap of  $\sim 20$  Å in the  $z$  direction normal to the  $xy$  plane was added to isolate the nanoplatelets from each other.[28] When performing the structure optimization ( $a_0$ ,  $b_0$ , and the positions of atoms), the  $c_0$  supercell lattice parameter remained fixed.

## III. RESULTS AND DISCUSSION

Two groups of causes that may result in appearance of spontaneous strain in Janus structures are expected. First, these are two bulk effects. The first of them is

TABLE I. Relative per-atom adsorption energies for F, Cl, and Br ligands in different positions on the (001) surface of a 4 ML thick CdSe nanoplatelet and the corresponding equilibrium lattice parameter. The energy of the structure with the lowest energy is taken as the reference point.

Configuration	F atoms		Cl atoms		Br atoms	
	$E$ (eV)	$a_0$ (Å)	$E$ (eV)	$a_0$ (Å)	$E$ (eV)	$a_0$ (Å)
bridge(1)	0.0	4.1457	0.0	4.1993	0.0	4.2157
bridge(2)	0.864	3.9289	0.766	4.0142	0.724	4.0521
atop	1.099	4.2425	0.959	4.2104	0.909	4.2105
hollow	1.311	3.8322	0.818	3.9205	0.699	3.9638

due to the difference in electronegativities of ligands, which results in a redistribution of the electron density and the appearance of (1) a vertical electric field in the nanoplatelet and (2) a shear strain of the supercell as a result of the inverse piezoelectric effect (we recall that bulk CdSe is a piezoelectric [27]). The second bulk effect is associated with the appearance of a vertical depolarizing field resulting from the difference in the potential jumps in the electrical double layers which appear when the positively charged nanoplatelet is covered with two different negatively charged  $X$ -type ligands at two sides. The second group of causes are various surface effects arising from mechanical stresses that appear upon formation of chemical bonds with ligands.

Because the effect of real ligands on the structure of nanoplatelets includes many aspects and may be very complex, the simplest monoatomic and diatomic ligands were used in our *ab initio* calculations to identify the mechanisms by which they influence the structure. This gives us a basis to classify the effects produced by more complex ligands.

### A. Monoatomic ligands

We start our study of the surface monoatomic ligands with the determination of their energetically most favorable positions. Different possible positions of adsorbed atoms on the (001) surface of zinc-blende structure are shown in Fig. 1b. It should be noted that in this structure there are two different types of bridging positions, bridge(1) and bridge(2). This follows from the fact that covalent chemical bond in zinc-blende structure is based on  $sp^3$  hybridized orbitals, and as a result of its directionality, the adsorption energies of atoms in these two positions are different. The relative adsorption energies of F, Cl, and Br atoms on the surface of a CdSe nanoplatelet are given in Table I. As was noted earlier [29], the most energetically favorable position of the ligand is the position, in which its local structure reproduces the structure of bulk CdSe. All other positions, including the bridge(2) one, have significantly higher energies. As follows from the obtained results, all considered ligands induce the

TABLE II. Stress  $\sigma_1$  in Janus CdSe nanoplatelets of various thicknesses  $N$  covered with F-Cl and Cl-Br ligand pairs. To unambiguously determine the sign of the stress, the more electronegative ligand atom in the nanoplatelet was always chosen to be the first one. The last column presents the  $a_0$  and  $b_0$  lattice parameters of the relaxed structure whose translation vector  $\mathbf{R}_1$  is directed along the bridging bond for a larger ligand.

$N$	$c_0$ (Bohr)	$\sigma_1$ (GPa)	$\sigma_1 c_0$	$a_0 = b_0$ (Å) (clamped)	$a_0, b_0$ (Å) (relaxed)
F and Cl ligands					
2	66.0	-0.3235	21.35	4.1139	4.2138, 4.0333
3	66.0	-0.3276	21.62	4.1509	4.2279, 4.0856
4	66.0	-0.3295	21.75	4.1729	4.2350, 4.1179
5	72.0	-0.3032	21.83	4.1867	4.2392, 4.1396
6	78.0	-0.2805	21.88	4.1968	4.2420, 4.1553
Cl and Br ligands					
2	66.0	-0.0794	5.24	4.1759	4.2003, 4.1518
3	66.0	-0.0792	5.23	4.1954	4.2138, 4.1769
4	66.0	-0.0793	5.23	4.2072	4.2224, 4.1925
5	72.0	-0.0727	5.24	4.2155	4.2281, 4.2031
6	78.0	-0.0672	5.24	4.2212	4.2320, 4.2105

in-plane contraction of the structure (in bulk CdSe, the calculated  $a_0 = a/\sqrt{2}$  value is 4.2550 Å).

To separate the surface effects from the bulk ones, the dependence of stresses created in nanoplatelets on their thickness  $N$  (given in monolayers) was studied. We focused our attention on stresses in order to exclude from consideration the elastic properties of nanoplatelets because they change with thickness. For this purpose, the calculations were carried out for nanoplatelets clamped on a square substrate ( $a_0 = b_0$ ) with the lattice parameter satisfying the boundary conditions  $\sigma_1 + \sigma_2 = 0$  (hereinafter, indices are given in Voigt notation). The parameter of interest to us was the stress  $\sigma_1 = -\sigma_2 \neq 0$ . The obtained results are given in Table II.[30]

When analyzing the obtained data, it should be taken into account that in the ABINIT program the stress is calculated as a force acting on the total surface area, which in structures containing a vacuum gap includes the area occupied by this layer [31]. This is why, when comparing data obtained on supercells of different lengths, it is more correct to use the product of the stress and the full period of the supercell in the  $z$  direction,  $\sigma_1 c_0$ . As follows from Table II, this value weakly depends on  $N$  and demonstrates a gradual saturation as the thickness of the nanoplatelet increases. A monotonous increase in the lattice parameter in clamped structures with increasing  $N$  confirms our earlier conclusion that all considered monoatomic ligands contract the structure.

Similar results were obtained for clamped CdSe Janus structures with surface Cl and Br ligands (Table II).

When the  $a_0 = b_0$  constraint is released, the structure relaxes and a noticeable spontaneous strain in the [110]

direction of the original cubic structure appears.[32] According to experiment, this direction coincides with the direction of spontaneous folding of nanoplatelets [8, 11] and their spontaneous strain [15]. The in-plane lattice parameters  $a_0$  and  $b_0$  of the orthorhombic relaxed structure are given in Table II. It is seen that as the thickness of the nanoplatelets increases, the magnitude of spontaneous strain decreases, which is explained by an increase in the mechanical rigidity of nanoplatelets (we note, however, that the elastic modulus  $C_{1212}$  is not a linear function of  $N$ ).

Judging from a very weak dependence of  $\sigma_1 c_0$  on the thickness of nanoplatelets, the perturbation source is localized. Unfortunately, the problem of separating the surface and bulk effects is complicated by the fact that in our geometry the Poisson's equation for the electric field is one-dimensional, and in the absence of screening (we are dealing with a semiconductor), the vertical electric field in the structure remains uniform. This is a direct consequence of the divergence theorem. In a long supercell, when the thickness of a semiconductor part of nanoplatelet changes, the lateral *pressure* produced by bulk electric field decreases, but the lateral *surface area* occupied by the semiconductor part increases, thus compensating each other. This makes it impossible to decide whether the observed spontaneous strain is caused by surface or bulk effects.

To separate these effects, additional calculations for two hypothetical structures were performed. The first of these was the nanoplatelet clamped on a square substrate with the atop position of both terminating atoms. In this configuration, the bulk effect associated with the difference in electronegativities of ligands should remain practically unchanged (ultimately, it is determined by the difference in energies of partially filled  $p$  orbitals in the ligands), and an anisotropic surface stresses that occur when the ligands are in bridge positions should disappear due to symmetry. For nanoplatelets with a thickness of 4 ML and surface atop F and Cl ligands, the obtained  $\sigma_1$  value was -0.0189 GPa, which was about 20 times less than in the configuration with bridging bonds (Table II). For nanoplatelets with a thickness of 3 ML and 5 ML, the calculations gave the values  $\sigma_1 = -0.0175$  GPa and  $\sigma_1 = -0.0172$  GPa, respectively. The sign of the effect remained the same as in the bridge(1) configuration. For a 4 ML thick nanoplatelet with atop Cl and Br ligands, the result was similar: the sign of the effect remained the same as in the bridge(1) configuration, but its magnitude was an order of magnitude smaller (-0.0060 GPa).

The second hypothetical structure was a clamped nanoplatelet with hollow positions of both ligands. In this structure, at a fixed thickness of the nanoplatelet, the vertical electric field resulting from the difference in electronegativities should remain almost the same as in the bridge(1) configuration, but the anisotropy of surface stresses should disappear due to symmetry. Calculations for a 4 ML thick nanoplatelets with the hollow positions of F and Cl ligands gave the value  $\sigma_1 = -0.0620$  GPa,

which turned out to be 3 times stronger than for the atop configuration. For nanoplatelets with a thickness of 3 ML and 5 ML, the  $\sigma_1$  values were  $-0.0355$  GPa and  $-0.0746$  GPa, respectively. The fact that the  $\sigma_1$  values in structures with atop and hollow positions are noticeably different indicates the existence of several competing bulk mechanisms. In our opinion, the second bulk mechanism is associated with a depolarizing electric field caused by different potential jumps in electrical double layers on two surfaces of nanoplatelets.

In an electrically neutral nanoplatelet, the positive charge of the semiconductor part is compensated by the negative charge of  $X$  ligands. In symmetric nanoplatelets, the potential jumps created by electrical double layers on two surfaces compensate each other and the bulk electric field is zero. However, in Janus nanoplatelets, these dipole moments do not compensate each other anymore, and an additional vertical electric field arises in the structure. This field, due to the inverse piezoelectric effect, creates additional mechanical stresses in the nanoplatelet. For example, in the 4 ML thick CdSe nanoplatelet, the distance between the layer of bridging F and Cl atoms and the nearest layers of cadmium atoms are  $0.689$  and  $1.352$  Å for the bridge(1) positions,  $1.934$  and  $2.269$  Å for atop positions, and  $0.619$  and  $1.075$  Å for the hollow positions. The corresponding differences in the interplanar Cd-F and Cd-Cl distances are  $0.663$ ,  $0.335$ , and  $0.456$  Å. A qualitative analysis of the distribution of fields created by the difference in electronegativities and by dipole moments on the surfaces of the nanoplatelet shows that the contribution of dipole moments should increase in the series atop-hollow-bridge(1), and its sign should coincide with the sign of the effect produced by the difference in electronegativities. This is exactly what is observed in our calculations.

The difference in the potential jumps on two sides of Janus nanoplatelets is clearly seen in the averaged electrostatic potential curves calculated for a special supercell containing two vacuum gaps and two oppositely oriented Janus nanoplatelets to suppress the depolarizing field (see Fig. S1 in the Supporting information). The potential curve was obtained using the macroaveraging technique [33] implemented in the `macroave` program of the ABINIT software package. It is seen that the difference in the potential jumps can be as large as  $0.77$  eV.

Displacements of atoms in a nanostructure from their ideal positions may provide additional information on the discussed phenomena. If one suppresses the strain by fixing the structure on a square substrate, the appearance of such displacements can indicate the presence of electric and stress fields in the structure. For example, the existence of a vertical electric field in clamped nanoplatelets with the bridge(1) position of ligands is confirmed by the observation of spatially uniform oscillations of interplanar distances (Fig. 2). Since the chemical bond in CdSe is partially ionic, this field acts on small positive and negative charges of atoms and results in out-of-phase displacements of the planes occupied by neighboring atoms. The direction of atomic displacements exactly corresponds to the direction of the electric field created by the difference in electronegativities.

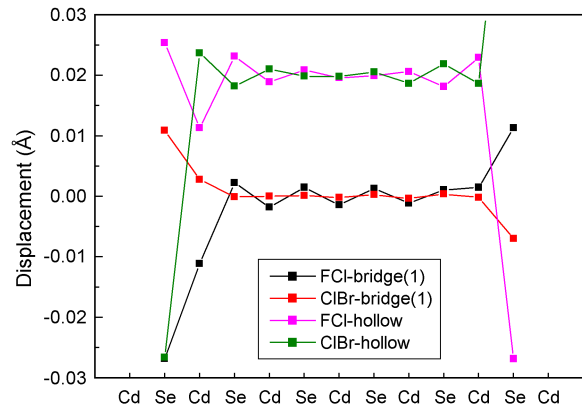


FIG. 2. Deviation of the  $z$  coordinates of individual atoms from the half-sum of the  $z$  coordinates of neighboring atoms in clamped 6 ML thick Janus CdSe nanoplatelets with F-Cl and Cl-Br ligand pairs (the more electronegative atom is located on the left). Two upper curves corresponding to the same ligand pairs in the hollow position are shifted by  $0.02$  Å for clarity.

ments of the planes occupied by neighboring atoms. The direction of atomic displacements exactly corresponds to the direction of the electric field created by the difference in electronegativities.

When ligands are moved to the atop and hollow positions, the character of the displacements changes. In particular, in a number of structures one can observe damped oscillations whose phase changes by  $180^\circ$  when passing to the other side of the nanoplatelet. To better understand the nature of the observed displacements, additional calculations were carried out for both conventional and Janus nanoplatelets made of silicon, a material in which the piezoelectric effect is absent. As follows from Fig. S2 of the Supporting information, similar displacement patterns were observed in fully symmetric Ge-terminated silicon nanoplatelets. Studies of Janus Si nanoplatelets with Ge and C terminating atoms show that these oscillations are induced by the nearest surface, and the sign of the displacements is determined by the sign of strain (compression or tension) at this surface. Therefore, oscillations of atomic displacements observed in CdSe nanoplatelets with a phase change by  $180^\circ$  point to the surface relaxation as the cause of this phenomenon. However, electrical effects cannot be completely ruled out since the surface piezoelectricity—the appearance of fields of piezoelectric origin in differently relaxed layers on the surface—can also play a certain role in CdSe nanoplatelets.

When the  $a_0 = b_0$  constraint is released, the structures with atop and hollow positions of ligands relax in the same way as the structures with the bridge(1) position, in accordance with the sign of  $\sigma_1$  in clamped structures. An analysis of the equilibrium geometry of the structures under discussion shows that the position of monoatomic

ligands on bridging bonds is always symmetric, and the Cd- $X$  bond lengths systematically increase in the series  $X = \text{F, Cl, Br}$ . This means that stress-free nanoplatelets always elongates in the direction of the bridging bond with a larger ligand.

The question can arise if the observed effects are entirely associated with the bulk electric field produced by the difference in the potential jumps at two surfaces of the nanoplatelet. Unfortunately, the dipole correction technique [34] is not implemented in the ABINIT package. In order to answer this question, we performed additional calculations for a number of doubled supercells containing two vacuum gaps and two oppositely oriented Janus nanoplatelets. It appeared that in these dipole-corrected calculations, the values of  $\sigma_1$  stress in clamped nanoplatelets are changed by no more than 2%. At the same time, the atomic displacements of Fig. 2 become weaker (see Fig. S3 in the Supporting information) and remind the atomic displacements patterns produced by the surface relaxation. The calculated profiles of the electrostatic potential show that without the dipole correction, the depolarizing electric field can reach 3 MV/cm in the vacuum layer and 200 kV/cm in the semiconductor part. In the supercells with suppressed depolarizing field, the weaker effect of the electric field originating from the difference in electronegativities of ligands is observed (see Fig. S4 in the Supporting information): its strength is about 30 kV/cm. A parabolic change of the potential in the middle of the nanoplatelet is due to homogeneous distribution of positive charge in the semiconductor part. It supports our model of the nanoplatelet as a positively charged semiconductor nanoplatelet covered with negatively charged  $X$  ligands.

To sum up this section, the performed calculations unambiguously indicate the existence of three microscopic mechanisms of spontaneous strain in Janus nanoplatelets. Two bulk mechanisms are associated with the inverse piezoelectric effect which occurs in an electric field created by different electronegativities of ligands and by different dipole moments of electrical double layers formed on two surfaces. These mechanisms account for 5–25% of the observed effect. The third mechanism is associated with the surface strain of nanoplatelets by bridging bonds, and its effect is predominant.

### B. Diatomic ligands

To better understand the mechanism of the surface strain, we now consider diatomic OH, SH, SeH, and TeH ligands in the bridge(1) position. It was shown that this position is the equilibrium one since structures with general starting positions of atoms relax into it. We start with the influence of geometric size of ligands on the magnitude of stresses in CdSe nanoplatelets clamped on a square substrate ( $a_0 = b_0, \sigma_1 + \sigma_2 = 0$ ). The results of calculations for a 4 ML thick nanoplatelet and various ligands paired with more electronegative F and Cl

TABLE III. Stress  $\sigma_1$  in 4 ML Janus CdSe nanoplatelets covered with various ligands. The translation vector  $\mathbf{R}_1$  is directed along the bridging bond of the  $Y$  ligand.

$Y$	$\sigma_1$ (GPa)	$R_{\text{Cd}-Y}$ (Å)	$a_0 = b_0$ (Å) (clamped)	$a_0, b_0$ (Å) (relaxed)
F and Y ligands				
OH	+0.0596	2.219	4.1126	4.1029, 4.1228
SH	-0.4021	2.504	4.1625	4.2333, 4.0931
SeH	-0.5162	2.618	4.1800	4.2733, 4.0924
TeH	-0.6336	2.749	4.2130	4.3278, 4.1114
Cl	-0.3295	2.486	4.1729	4.2350, 4.1179
Br	-0.4108	2.601	4.1817	4.2602, 4.1141
COO	-0.5846	2.190 <sup>a</sup>	4.2039	4.3089, 4.1110
Cl and Y ligands				
OH	+0.3918	2.224	4.1387	4.0755, 4.2141
SH	-0.0644	2.506	4.1882	4.1997, 4.1757
SeH	-0.1767	2.620	4.2055	4.2378, 4.1717
TeH	-0.2909	2.750	4.2378	4.2904, 4.1844
F	+0.3295	2.197	4.1729	4.1179, 4.2350
Br	-0.0793	2.603	4.2072	4.2224, 4.1925

<sup>a</sup>In contrast to the results of Ref. 35, our calculations show that the most stable configuration of the HCOO ligand is its tilted configuration. The table presents the shortest Cd-O distance.

ligands are given in Table III.

It is seen that when passing from OH to larger ligands, the  $\sigma_1$  stress changes its sign from positive to negative, and its negative values continue to increase with increasing ligand size. This fully supports the idea of the surface stress as a mechanism of the influence of ligands on spontaneous strain. The OH ligand causes contraction of the structure in the direction of the bridging bond, whereas all other ligands elongate it in accordance with the bond length  $R_{\text{Cd}-Y'}$  ( $Y' = \text{O, S, Se, Te}$ ). Calculations show that the  $Y'$  atoms that occupy the bridge position remain at an equal distance from the Cd atoms, but the inclination of the  $Y'$ -H bond, which is accompanied by slight opposite lateral shifts of the  $Y'$  and H atoms in the direction perpendicular to the bridging bond, results in a distortion of the structure. It lowers its symmetry to  $Pm$ .

The atomic displacements in the  $y$  direction produced by distortion of the surface by different diatomic ligands are shown in Fig. 3. It is seen that in the bulk of a semiconductor the atomic displacements rapidly decay with distance. This indicates the surface origin of the perturbation. However, the origin of the displacement oscillations deep in structure turns out to be quite unexpected: for all ligands, an analysis finds a doubled character of displacements of neighboring atoms, thus indicating the involvement of TA phonon at the  $X$  point of the Brillouin zone, which has a similar eigenvector, into the relaxation. The observed doubling is typical of zinc-blende structure,

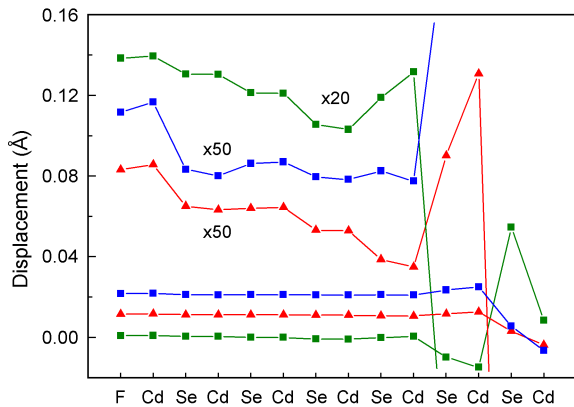


FIG. 3. Damping of atomic  $y$  displacements in the bulk of a clamped 6 ML thick Janus CdSe nanoplatelet caused by the surface displacement of the hydrogen atom in OH (green squares), SH (red triangles), and SeH (blue squares) groups. The top three curves show enlarged displacement patterns inside the nanoplatelet.

in which vibrations of Cd–Se pairs in the  $[110]$  direction alternately become stretching, then bending, then stretching again. Weak additional out-of-phase displacements of Cd and Se atoms may indicate the existence of an electric field parallel to the surface.

Similar results were also obtained for 4 ML thick Janus CdSe nanoplatelets with OH, SH, SeH, and TeH ligands in the bridge(1) position in a pair with a more electronegative Cl atom (Table III).

By comparing data for diatomic ligands with the results obtained for monoatomic ligands, one can conclude that the surface contribution to spontaneous strain is determined by the difference in geometric size of ligands. Based on the lattice parameters of clamped structures at  $\sigma_1 + \sigma_2 = 0$  (Table III), the ligands can be arranged in the following series according to their strain effect: OH–F–Cl–SH–Br–SeH–TeH. For all ligands we have considered, the absolute sign of the strain is negative, which follows from the comparison of obtained  $a_0$  parameters with that calculated for bulk CdSe ( $a_0 = a/\sqrt{2} = 4.2550 \text{ \AA}$ ). Alternatively, the  $\sigma_1$  values can be used to evaluate the effect of ligands on the spontaneous strain.

The geometry of CdSe nanoplatelets is such that regardless of whether they have an even or odd number of monolayers, the directions of bridging bonds on their two opposite sides are always perpendicular to each other. When the monoatomic ligands are the same and we use a 3D modeling program, this guarantees the preservation of the tetragonal structure. However, in Janus structures, the symmetry becomes lower. In the case of diatomic ligands, the situation is additionally complicated by the appearance of a transverse component of atomic displacements.

Unfortunately, the 3D modeling programs do not allow to change the unit cell parameters when moving along

the  $z$  axis and thus do not allow one to clearly see what will happen with a free-standing 2D nanoplatelet. However, this is not hard to imagine. If we change to a curvilinear coordinate system, in which the  $x$  and  $y$  axes run parallel to the atomic chains on the surface and the  $z$  axis is directed perpendicular to them, then the mechanism of surface strain established above will result in a bending of the structure, and the interatomic distances in chains along the  $x$  and  $y$  axes will become  $z$ -dependent.

Anisotropic compressive stresses directed perpendicular to each other at two sides of a nanoplatelet will result in a saddle-shaped distortion of Janus nanoplatelets with small lateral sizes and will be characterized by two radii of principal curvatures. To be able to roll up nanoplatelets with a large lateral size into scrolls, one of the curvatures should be close to zero (the experiment shows that in most CdSe-based nanostructures the product of the two principal curvatures—so-called Gaussian curvature—is zero [8]). If so, then the belt- or ribbon-type nanostructures oriented in the  $[110]$  direction will form scrolls, whereas nanostructures oriented in the  $[100]$  direction will form spirals. When the curvatures of  $[100]$ -oriented ribbons are close, the formation of a twisted-ribbon structure becomes possible.

In this work, we did not plan to discuss the properties of nanoplatelets covered with long-chain organic molecules, since we were mainly interested in studying the structure of the interface between a semiconductor and ligands and the mechanisms that govern it. For organic ligands, the problem becomes more difficult since one of the oxygen atoms of the carboxyl group that forms a chemical bond occupies a distorted bridge(1) position with three different Cd–O distances. So, the surface distortions become even more complex and an additional problem arises, which requires to take into account the strain interaction in the layer of organic molecules. According to our calculations, the geometric size of the carboxyl group, judging from its effect on the lattice parameter, is slightly smaller than that of the TeH ligand (Table III).

Returning back to the phenomenon of spontaneous folding of nanoplatelets, we note that one of the puzzles in explaining this phenomenon is why it appears when both sides of the nanoplatelet are covered with ligands symmetrically. But if we assume that Janus nanoplatelets spontaneously occur in a colloidal solution, then an increase in the equilibrium lattice parameter in these nanoplatelets that arises when a larger ligand is placed on one of its sides should obviously result in such a folding.[36] This may occur, for example, as a result of the ordering of oleic and acetate groups on two sides of nanoplatelets (according to NMR [35], nanoplatelets synthesized using lead acetate usually contain both types of groups). The stability of such configurations is ensured by the Gorsky effect (diffusional exchange of ligands in a stress field). Indirect evidences for formation of Janus structures can be observed in refs. 13–15, 37, in which the distance between layers in nanoplatelets rolled into scrolls

as well as in nanotubes are markedly less than twice the length of the long-chain organic stabilizer molecules (about 22 Å for oleic acid and hexadecanethiol). This may indicate the appearance of short-chain organic ligands in combination with the long-chain ones in the gap. It should also be noted that spontaneous strain along the [110] direction is typical of Janus nanoplatelets: according to our calculations, nanoplatelets covered on both sides with the same organic ligands spontaneously strain in the [100] direction.

To estimate the curvature radius of a rolled nanostructure, one can use the  $a_0$  and  $b_0$  values from Table II, although for a real free-standing nanoplatelet, the difference between these parameters can be even stronger. For a 3 ML thick nanoplatelet, the characteristic radius of curvature is  $\sim 36$  nm and agrees with experiment.

#### IV. CONCLUSIONS

The first-principles calculations of the geometry of Janus CdSe nanoplatelets performed in this work indicate the existence of three microscopic mechanisms of their spontaneous strain. Two bulk mechanisms are associated with the inverse piezoelectric effect in an electric field created by the difference in electronegativities of ligands and in the depolarizing field resulting from the difference in the potential jumps in electrical double layers on two surfaces of nanoplatelets. These mechanisms account for 5–25% of the observed effect. The third mechanism is due to the surface strain of the nanoplatelet by bridging bonds, and its effect is predominant. The latter mechanism initiates spontaneous folding of thin nanoplatelets and, depending on the magnitude of surface stresses and orientation of nanoplatelets in the lateral plane, can result in formation of scrolls, spirals, or twisted ribbons.

#### Appendix A: Supporting information

Fig. S1 shows the averaged electrostatic potential calculated using the `macroave` program from the `ABINIT` software package for a dipole-corrected structure consisting of two vacuum gaps and two oppositely oriented clamped F- and Cl-terminated Janus 8 ML-thick CdSe nanoplatelets. It is seen that in two vacuum layers, the electrostatic potentials which result from the difference in the potential jumps in electrical double layers at the surfaces of each nanoplatelet, differ by 0.77 eV. In structures without the dipole correction, this difference in the potential jumps was shown to induce the depolarizing fields up to 3 MV/cm in the vacuum region and up to 200 kV/cm in the semiconductor part.

The deviations of the  $z$  coordinates of individual atoms from the half-sum of the  $z$  coordinates of neighboring atoms in a clamped 31 ML-thick silicon nanoplatelet symmetrically terminated with Ge atoms are shown in Fig. S2. One can see an interference of damped oscil-

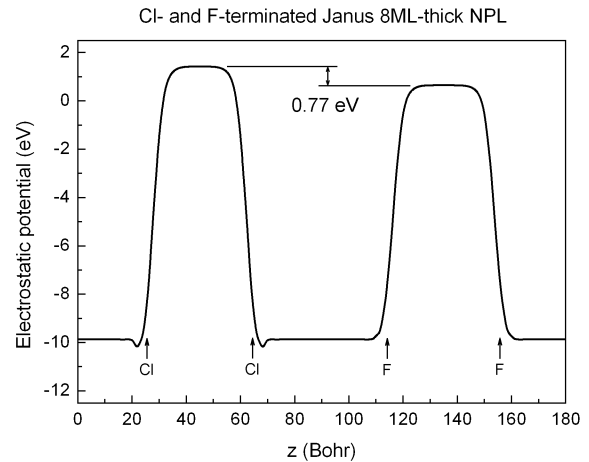


FIG. S1. Averaged electrostatic potential in dipole-corrected structure consisting of two vacuum gaps and two oppositely oriented clamped F- and Cl-terminated Janus 8 ML-thick CdSe nanoplatelets.

lations which have a phase shift of  $180^\circ$  and come from two opposite sides of the nanoplatelet. The origin of this structure is the surface relaxation.

Fig. S3 shows the effect of the dipole correction on the deviation of the  $z$  coordinates of individual atoms from the half-sum of the  $z$  coordinates of neighboring atoms in a clamped 8 ML-thick Janus CdSe nanoplatelet terminated by F and Cl ligands. It is seen that without the dipole correction, the depolarizing field induces, via the inverse piezoelectric effect, large out-of-phase shifts of Cd and Se atoms. When the depolarizing field are switched off by using a special supercell with two vacuum gaps and two oppositely oriented Janus nanoplatelets, the oscillations become much weaker and display a picture of two interfering damped waves coming from two opposite sides of the nanoplatelet and having the  $180^\circ$  phase shift typical of the surface relaxation (Fig. S2).

Fig. S4 presents an enlarged portion of the averaged electrostatic potential of Fig. S1 inside the nanoplatelet. As the nanoplatelet is mechanically clamped and the depolarizing field is fully compensated, the only remaining perturbation is the electric field induced by the difference in electronegativities of ligands. It produces a change of the averaged electrostatic potential with a slope of  $\sim 30$  kV/cm. A parabolic change of the potential in the middle of the nanoplatelet is due to homogeneous distribution of positive charge in the semiconductor part. It supports its model as a positively charged semiconductor nanoplatelet covered with negatively charged  $X$  ligands.

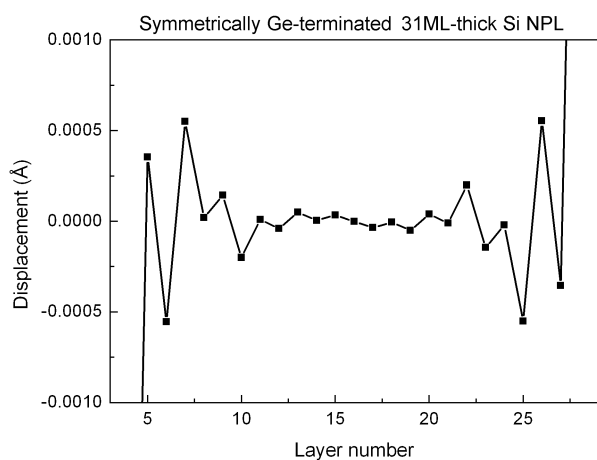


FIG. S2. Deviations of the  $z$  coordinates of individual atoms from the half-sum of the  $z$  coordinates of neighboring atoms in clamped 31 ML-thick silicon nanoplatelet terminated with Ge atoms.

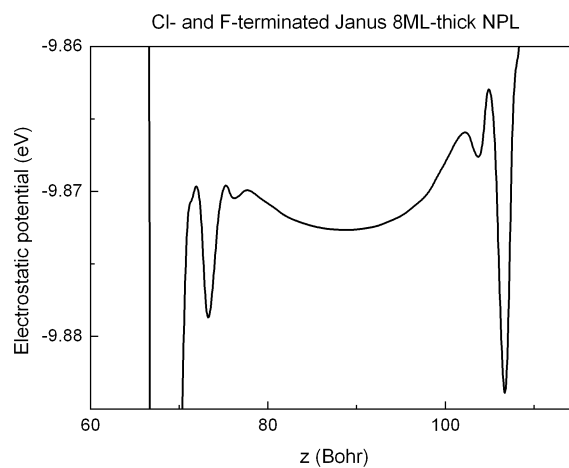


FIG. S4. Enlarged portion of Fig. S1 showing the profile of the averaged electrostatic potential inside the nanoplatelet.

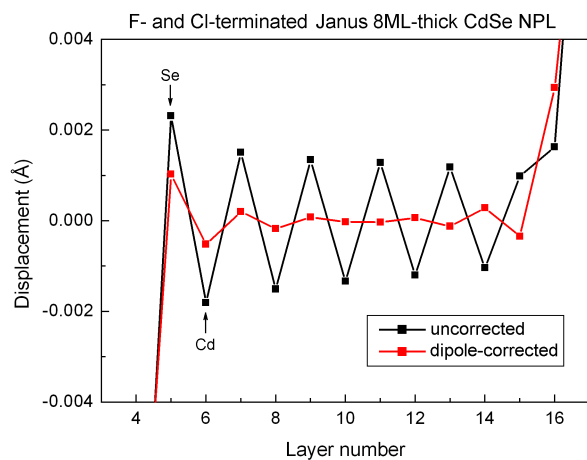


FIG. S3. Deviations of the  $z$  coordinates of individual atoms from the half-sum of the  $z$  coordinates of neighboring atoms in clamped 8 ML-thick Janus CdSe nanoplatelet terminated with F and Cl ligands before and after the dipole correction.

## ACKNOWLEDGMENTS

The work was financially supported by Russian Science Foundation, grant 22-13-00101. The author thanks R.B. Vasiliev who stimulated the author's interest to nanoplatelets for numerous fruitful discussions of various aspects of the problem.

- 
- [1] C. Bouet, M. D. Tessier, S. Ithurria, B. Mahler, B. Nadal, and B. Dubertret, Flat colloidal semiconductor nanoplatelets, *Chem. Mater.* **25**, 1262 (2013).
- [2] M. Nasilowski, B. Mahler, E. Lhuillier, S. Ithurria, and B. Dubertret, Two-dimensional colloidal nanocrystals, *Chem. Rev.* **116**, 10934 (2016).
- [3] B. T. Diroll, B. Guzelturk, H. Po, C. Dabard, N. Fu, L. Makke, E. Lhuillier, and S. Ithurria, 2D II–VI semiconductor nanoplatelets: From material synthesis to optoelectronic integration, *Chem. Rev.* **123**, 3543 (2023).
- [4] S. Ithurria, M. D. Tessier, B. Mahler, R. P. S. M. Lobo, B. Dubertret, and A. L. Efros, Colloidal nanoplatelets with two-dimensional electronic structure, *Nat. Mater.* **10**, 936 (2011).
- [5] A. Naeem, F. Masia, S. Christodoulou, I. Moreels, P. Borri, and W. Langbein, Giant exciton oscillator strength and radiatively limited dephasing in two-dimensional platelets, *Phys. Rev. B* **91**, 121302 (2015).
- [6] C. She, I. Fedin, D. S. Dolzhenkov, A. Demortière, R. D. Schaller, M. Pelton, and D. V. Talapin, Low-threshold stimulated emission using colloidal quantum wells, *Nano Lett.* **14**, 2772 (2014).
- [7] J. Q. Grim, S. Christodoulou, F. Di Stasio, R. Krahne, R. Cingolani, L. Manna, and I. Moreels, Continuous-wave biexciton lasing at room temperature using solution-processed quantum wells, *Nat. Nanotechnol.* **9**, 891 (2014).
- [8] L. Guillemeney, L. Lermusiaux, G. Landaburu, B. Wagnon, and B. Abécassis, Curvature and self-assembly of semi-conducting nanoplatelets, *Commun. Chem.* **5**, 7 (2022).
- [9] S. Ithurria and B. Dubertret, Quasi 2D colloidal CdSe platelets with thicknesses controlled at the atomic level, *J. Am. Chem. Soc.* **130**, 16504 (2008).
- [10] B. Mahler, B. Nadal, C. Bouet, G. Patriarche, and B. Dubertret, Core/shell colloidal semiconductor nanoplatelets, *J. Am. Chem. Soc.* **134**, 18591 (2012).
- [11] C. Bouet, B. Mahler, B. Nadal, B. Abécassis, M. D. Tessier, S. Ithurria, X. Xu, and B. Dubertret, Two-dimensional growth of CdSe nanocrystals, from nanoplatelets to nanosheets, *Chem. Mater.* **25**, 639 (2013).
- [12] R. B. Vasiliev, M. S. Sokolikova, A. G. Vitukhnovskii, S. A. Ambrozevich, A. S. Selyukov, and V. S. Lebedev, Optics of colloidal quantum-confined CdSe nanoscrolls, *Quant. Electron.* **45**, 853 (2015).
- [13] N. N. Schlenskaya, Y. Yao, T. Mano, T. Kuroda, A. V. Garshev, V. F. Kozlovskii, A. M. Gaskov, R. B. Vasiliev, and K. Sakoda, Scroll-like alloyed  $\text{CdS}_x\text{Se}_{1-x}$  nanoplatelets: Facile synthesis and detailed analysis of tunable optical properties, *Chem. Mater.* **29**, 579 (2017).
- [14] R. B. Vasiliev, E. P. Lazareva, D. A. Karlova, A. V. Garshev, Y. Yao, T. Kuroda, A. M. Gaskov, and K. Sakoda, Spontaneous folding of CdTe nanosheets induced by ligand and exchange, *Chem. Mater.* **30**, 1710 (2018).
- [15] D. A. Kurtina, A. V. Garshev, I. S. Vasil'eva, V. V. Shubin, A. M. Gaskov, and R. B. Vasiliev, Atomically thin population of colloidal CdSe nanoplatelets: Growth of rolled-up nanosheets and strong circular dichroism induced by ligand exchange, *Chem. Mater.* **31**, 9652 (2019).
- [16] N. Castro, C. Bouet, S. Ithurria, N. Lequeux, D. Constantin, P. Levitz, D. Pontoni, and B. Abécassis, Insights into the formation mechanism of CdSe nanoplatelets using in situ X-ray scattering, *Nano Lett.* **19**, 6466 (2019).
- [17] H. Po, C. Dabard, B. Roman, E. Reyssat, J. Bico, B. Baptiste, E. Lhuillier, and S. Ithurria, Chiral helices formation by self-assembled molecules on semiconductor flexible substrates, *ACS Nano* **16**, 2901 (2022).
- [18] E. M. Hutter, E. Bladt, B. Goris, F. Pietra, J. C. van der Bok, M. P. Boneschanscher, C. de Mello Donegá, S. Bals, and D. Vanmaekelbergh, Conformal and atomic characterization of ultrathin CdSe platelets with a helical shape, *Nano Lett.* **14**, 6257 (2014).
- [19] M. Dufour, J. Qu, C. Greboval, C. Méthivier, E. Lhuillier, and S. Ithurria, Halide ligands to release strain in cadmium chalcogenide nanoplatelets and achieve high brightness, *ACS Nano* **13**, 5326 (2019).
- [20] S. Jana, M. de Frutos, P. Davidson, and B. Abécassis, Ligand-induced twisting of nanoplatelets and their self-assembly into chiral ribbons, *Sci. Adv.* **3**, e1701483 (2017).
- [21] N. V. Tepliakov, A. S. Baimuratov, I. A. Vovk, M. Y. Leonov, A. V. Baranov, A. V. Fedorov, and I. D. Rukhlenko, Chiral optical properties of tapered semiconductor nanoscrolls, *ACS Nano* **11**, 7508 (2017).
- [22] A.-Y. Lu, H. Zhu, J. Xiao, C.-P. Chuu, Y. Han, M.-H. Chiu, C.-C. Cheng, C.-W. Yang, K.-H. Wei, Y. Yang, Y. Wang, D. Sokaras, D. Nordlund, P. Yang, D. A. Muller, M.-Y. Chou, X. Zhang, and L.-J. Li, Janus monolayers of transition metal dichalcogenides, *Nat. Nanotechnol.* **12**, 744 (2017).
- [23] A. I. Lebedev, B. M. Saidzhonov, K. A. Drozdov, A. A. Khomich, and R. B. Vasiliev, Raman and infrared studies of CdSe/CdS core/shell nanoplatelets, *J. Phys. Chem. C* **125**, 6758 (2021).
- [24] X. Gonze, B. Amadon, P.-M. Anglade, J.-M. Beuken, F. Bottin, P. Boulanger, F. Bruneval, D. Caliste, R. Caracas, M. Côté, T. Deutsch, L. Genovese, P. Ghosez, M. Giantomassi, S. Goedecker, D. R. Hamann, P. Hermet, F. Jollet, G. Jomard, S. Leroux, M. Mancini, S. Mazevet, M. J. T. Oliveira, G. Onida, Y. Pouillon, T. Rangel, G.-M. Rignanese,

- D. Sangalli, R. Shaltaf, M. Torrent, M. J. Verstraete, G. Zerah, and J. W. Zwanziger, ABINIT: First-principles approach to material and nanosystem properties, *Computer Phys. Commun.* **180**, 2582 (2009).
- [25] A. M. Rappe, K. M. Rabe, E. Kaxiras, and J. D. Joannopoulos, Optimized pseudopotentials, *Phys. Rev. B* **41**, 1227 (1990).
- [26] Opium—pseudopotential generation project, <http://opium.sourceforge.net/> (accessed April 26, 2023).
- [27] S. Adachi, *Properties of Semiconductor Alloys: Group-IV, III-V and II-VI Semiconductors* (John Wiley & Sons Ltd., 2009).
- [28] In reality, the nanoplatelet under consideration has a symmetry of the  $p\bar{4}m2$  layer group. The possibility of its modeling using 3D modeling programs within the  $P\bar{4}m2$  space group was discussed in Ref. 23.
- [29] R. B. Vasiliev, A. I. Lebedev, E. P. Lazareva, N. N. Shlenskaya, V. B. Zaytsev, A. G. Vitukhnovsky, Y. Yao, and K. Sakoda, High-energy exciton transitions in quasi-two-dimensional cadmium chalcogenide nanoplatelets, *Phys. Rev. B* **95**, 165414 (2017).
- [30] The boundary conditions depend on the orientation of the unit cell. For example, for the unit cell with the  $[a/2, a/2, 0]$ ,  $[-a/2, a/2, 0]$ ,  $[0, 0, c_0]$  translation vectors, the boundary condition are  $\sigma_1 = \sigma_2 = 0$ , and the stress in question is  $\sigma_6$ .
- [31] A. I. Lebedev, Ferroelectricity and piezoelectricity in monolayers and nanoplatelets of SnS, *J. Appl. Phys.* **124**, 164302 (2018).
- [32] In our supercell setting, the relaxation of the structure produced by the stress  $\sigma_1 = -\sigma_2 \neq 0$  results in a change of lengths of the translation vectors,  $a_0 \neq b_0$ .
- [33] A. Baldereschi, S. Baroni, and R. Resta, Band offsets in lattice-matched heterojunctions: A model and first-principles calculations for GaAs/AlAs, *Phys. Rev. Lett.* **61**, 1734 (1988).
- [34] L. Bengtsson, Dipole correction for surface supercell calculations, *Phys. Rev. B* **59**, 12301 (1999).
- [35] J. Zhang, H. Zhang, W. Cao, Z. Pang, J. Li, Y. Shu, C. Zhu, X. Kong, L. Wang, and X. Peng, Identification of facet-dependent coordination structures of carboxylate ligands on CdSe nanocrystals, *J. Am. Chem. Soc.* **141**, 15675 (2019).
- [36] Bulk effects can only result in spontaneous strain of the nanoplatelet without giving rise to its spontaneous folding.
- [37] X. Huang, V. K. Parashar, and M. A. M. Gijs, Spontaneous formation of CdSe photoluminescent nanotubes with visible-light photocatalytic performance, *ACS Cent. Sci.* **5**, 1017 (2019).